NISTR
QC100
.U5753
no. 1327
1989

# Radiometer Equation and Analysis of Systematic Errors for the NIST Automated Radiometers

**William C. Daywitt**

Electromagnetic Fields Division
Center for Electronics and Electrical Engineering
National Engineering Laboratory
National Institute of Standards and Technology
Boulder, Colorado 80303-3328

U.S. DEPARTMENT OF COMMERCE, Robert A. Mosbacher, Secretary
Ernest Ambler, Acting Under Secretary for Technology
NATIONAL INSTITUTE OF STANDARDS AND TECHNOLOGY, Raymond G. Kammer, Acting Director

Issued March 1989

National Institute of Standards and Technology Technical Note 1327
Natl. Inst. Stand. Technol., Tech Note 1327, 28 pages (Mar. 1989)
CODEN:NTNOEF

U.S. GOVERNMENT PRINTING OFFICE
WASHINGTON: 1989

For sale by the Superintendent of Documents, U.S. Government Printing Office, Washington, DC 20402-9325

## CONTENTS


Page

1. Introduction ..... 1
2. Radiometer Equation ..... 2
3. Cryogenic Standard Error ..... 5
4. Ambient Standard Error ..... 5
5. Power Ratio Error ..... 6
6. Mismatch Factor Error ..... 6
7. Asymmetry Measurement and Error ..... 7
8. Isolation Error ..... 10
9. Connector Error ..... 12
10. Frequency Offset Error ..... 14
11. Nonlinearity Error ..... 14
12. Total Error ..... 17
13. Summary, Discussion, and Conclusions ..... 18
14. Acknowledgments ..... 19
15. References ..... 21

# Radiometer Equation and Analysis of Systematic Errors for the NIST Automated Radiometers

*W.C. Daywitt*

Equations used in the NIST coaxial and waveguide automated radiometers to estimate the noise temperature and associated errors of a single-port noise source are derived in this report. These equations form the foundation upon which the microwave and millimeterwave noise calibration and special test services are performed. Results from the 1-12 GHz coaxial radiometer are presented.

Key words: calibration; error analysis; microwave; millimeterwave; noise temperature; radiometer.

## 1. Introduction

The Electromagnetic Fields Division of the National Institute of Standards and Technology (NIST) has two types of radiometers in operation at the present time, the switching and total-power radiometers. The radiometer and error analysis equations for the WR90 and WR62 switching radiometers have been previously described [1]. Similar equations for the automated, total-power radiometers are derived in this report. These radiometers are designed to provide noise temperature calibrations and special test services for coaxial and waveguide noise sources. The coaxial radiometer operates from 1 to 12 GHz in the following frequency ranges: 350 MHz to 500 MHz, 500 MHz to 1 GHz, 1 to 2 GHz, 2 to 4 GHz, 4 to 8 GHz, and 8 to 12 GHz; a separate r.f. front end being supplied for each of these ranges. Results from the 2 to 4 GHz range will be presented in this report. The hardware and software aspects of the coaxial radiometer is presented in [2].

The millimeterwave radiometers are under construction, and consist of the WR10, WR15, WR22, WR28, and WR42 waveguide bands.

A simplified schematic diagram of the system is shown in figure 1, where the directional coupler, isolator, r.f. amplifier, and mixer represent any one of the front ends just mentioned, while the 6-port circuitry is common to all frequency ranges. The system performs two functions. With the switch in the 'up' position as shown in the diagram it operates as a radiometer with the measurement sequence determining both the effective input noise temperature [3] $T_e$ of the system and the noise temperature $T_x$ of the DUT (device under test) by comparison against the ambient $T_a$ and cryogenic $T_s$ noise temperature standards. With the switch in the 'down' position it operates as a single 6-port, vector reflectometer for determining the complex reflection coefficients of the DUT, the standards, and the input port of the system. In the radiometer mode, switches at the system input (not shown in the diagram) alternately sample the noise temperatures $T_s$, $T_a$, and $T_x$ at which time their respective down-converted, i.f. powers are determined by the detector. An estimate of $T_x$ is made by inserting ratios of these powers and the reflection coefficients into a radiometer equation. A derivation of this radiometer equation along with the associated errors is the subject of this report, and is based upon analytical tools to be found elsewhere in the literature [4], [5].

## 2. Radiometer Equation

A theoretical examination of the measurement technique leads to an equation relating 1) the various power and reflection coefficient measurements made with the system to 2) the noise temperature of the DUT and the two noise standards. When this equation is solved for the noise temperature $T_x$ of the DUT there results an equation which for convenience is called the *radiometer equation.* Figure 2 is a schematic diagram of that portion of the system needed for the analysis, consisting of a front end between the noise sources $T_x$ and $T_s$, and the switch at the receiver and 6-port inputs. This switch following the isolator is set to the receiver position for the noise and asymmetry measurements, or to the 6-port reflectometer for the reflection measurements. The front end switches (22 through 25 in the diagram) correspond to the identically numbered switches in figure 3 of the operating manual [2]. The net i.f. powers $P_x$, $P_a$, and $P_s$ detected by the power meter are related to the r.f. spectral powers [3] $p_x$, $p_a$, and $p_s$ by the equation

$$P_i = gBp_i \qquad (i = x, a, s) \tag{2.1}$$

where $g$ is the system gain at the measurement frequency and $B$ is the system noise (or convolution [6]) bandwidth. The gain-bandwidth product in (2.1) will be dropped since only power ratios are needed in the following analysis, and Boltzmann's constant is set equal to unity in the following so that spectral powers and noise temperatures may be used interchangably. When the DUT is connected to the system input at switch 25, and switches 22 and 23 are in their 'up' positions, the spectral power delivered to the receiver is

$$p_x = M_x T_x \eta_x + T_a(N_x - M_x \eta_x) + N_x T_e \tag{2.2}$$

where $M_x$ and $N_x$ are mismatch factors [4] at the ports indicated in the figure for different switch positions, $\eta_x$ is the efficiency of the front end from port 3 to the isolator output, $T_a$ is the ambient temperature of the switches, and $T_e$ is the effective input noise temperature of the receiver and power meter combination. The second term in (2.2) accounts for the thermal noise generated in the switches and the isolator.

When switch 22 is in the 'down' position, the power is

$$p_a = N_a T_a + N_a T_e. \tag{2.3}$$

With switches 23 and 24 'down' and switch 22 'up' the power is

$$p_s = M_s T_s \eta_s + T_a(N_s - M_s \eta_s) + N_s T_e. \tag{2.4}$$

The following ratios are calculated from the measured powers;

$$Y_x = p_x / p_a \tag{2.5}$$

and

$$Y_s = p_s / p_a. \tag{2.6}$$

Equations (2.3) through (2.6) can then be combined and lead to

$$\mathbf{T_x = T_a + (M_s \eta_s / M_x \eta_x)[(Y_x - 1)/(Y_s - 1)](T_s - T_a) + (\Delta T_x)_{ISO}} \tag{2.7}$$

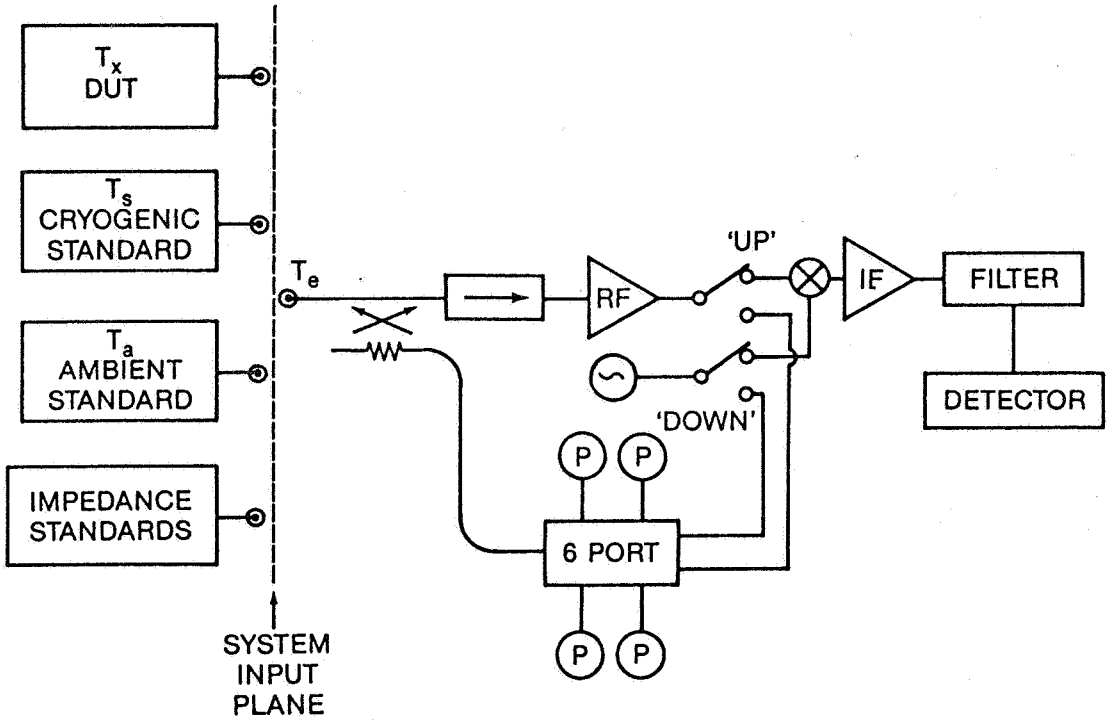


**Figure 1.** A simplified schematic diagram of the automated radiometer.

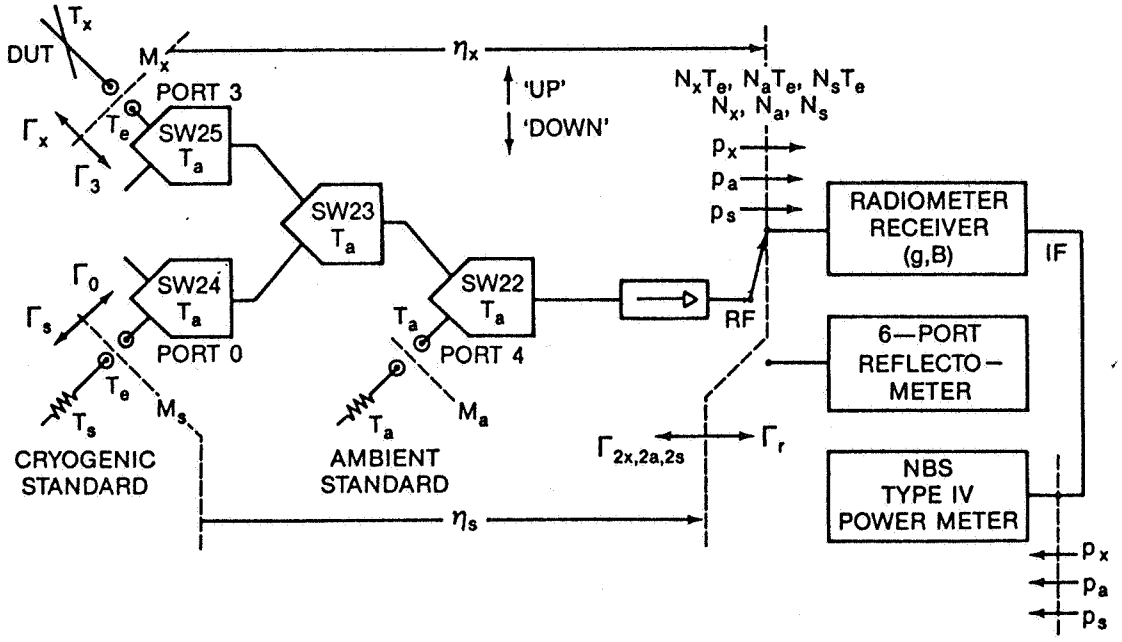


**Figure 2.** A schematic diagram of the automated radiometer's r.f. front end.

where the last term is an uncertainty due to the finite isolation of the isolator in figure 2. This error is a result of the different impedances seen by the receiver as the system samples power from the three noise sources. This changing impedance affects both the spectral powers and the value of the receiver noise temperature as reflected in the equation

$$(\Delta T_x)_{ISO} = (\Delta T_x)_N + (\Delta T_x)_e \tag{2.8}$$

where

$$(\Delta T_x)_N = (T_a/M_x\eta_x)[(Y_x - 1)(N_s - N_a)/(Y_s - 1) + N_a - N_x] \tag{2.9}$$

and

$$(\Delta T_x)_e = (1/M_x\eta_x)[(Y_x - 1)/(Y_s - 1)](N_sT_e - N_aT_e). \tag{2.10}$$

The boldfaced portion of (2.7) (i.e. without the isolator error term) is the *radiometer equation* that relates the DUT noise temperature $T_x$ to the ambient and cryogenic noise temperatures ($T_a$ and $T_s$) and the measured Y-factor ratios and mismatch factors. More explicit expressions for the $M$'s, $\eta$'s, $(\Delta T_x)_{ISO}$, $T_s$ and $T_a$ will be developed later.

Although the effective input noise temperature $T_e$ and the system gain $g$ are not needed in the radiometer equation, these parameters are monitored to help validate system performance. The Y-factor technique [7] is used to obtain a rough estimate of the effective input noise temperature of the system at the receiver input in figure 2 by switching between the cryogenic and ambient noise standards. The derivation is straightforward and leads to

$$T_e = (T_a - YT_s)/(Y - 1) \tag{2.11}$$

where $Y$ is the measured ratio of: 1) the spectral power with the ambient source connected to the system input; to 2) the spectral power with the cryogenic source connected to the system. The front-end switches are assumed to be lossless and reflectionless for this estimate.

An approximate value for the system gain is also of interest and can be obtained from

$$g = P_a/k(T_a + T_e)\,B \tag{2.12}$$

where $P_a$ is the power at the power meter with switch 22 in the 'down' position, and $k$ is Boltzmann's constant. The noise bandwidth $B$ is measured before the radiometer measurement, and is stored in the system software for use in (2.12).

## 3. Cryogenic Standard Error

The DUT noise temperature error $\delta T_x$ due to an uncertainty $\delta T_s$ in the cryogenic standard is found by differentiating the radiometer equation with respect to $T_s$, multiplying the result by $\delta T_s$, and discarding $M_s/M_x$ and $\eta_s/\eta_x$ since these two factors are close to unity. The corresponding relative error $\mathcal{E}_s$ in the DUT noise temperature is

$$\mathcal{E}_s \equiv \delta T_x/T_x = (T_s/T_x) \mid (T_x - T_a)/(T_s - T_a) \mid (\delta T_s/T_s). \tag{3.1}$$

The last factor is the relative uncertainty in the standard noise temperature, and takes a different form for the coaxial [8a] and waveguide [8b] noise standards.

The relative noise temperature uncertainty of the coaxial standard for frequencies between 1 and 12.4 GHz is [8a]

$$\delta T_s/T_s = \binom{+0.23}{-0.29} + [\binom{+0.19}{-0.12} \pm 0.05 \mid \Gamma_s \mid] f^{1/2} \pm 0.0036 f \ \ \% \tag{3.2}$$

where $f$ is the frequency in GHz, and $\Gamma_s$ is the reflection coefficient of the standard.

## 4. Ambient Standard Error

Ignoring the mismatch factors and asymmetry ratio in the radiometer equation shows that an uncertainty of $\delta T_a$ in the ambient standard output leads to a relative error $\mathcal{E}_a$ of

$$\mathcal{E}_a = (T_a/T_x) \mid 1 - (T_x - T_a)/(T_s - T_a) \mid (\delta T_a/T_a) \tag{4.1}$$

where $\delta T_a/T_a$ is the relative uncertainty in the ambient standard output. With an assumed value of $\pm 0.25$ K for $\delta T_a$ and a nominal value of 297 K for $T_a$,

$$\delta T_a/T_a = 0.17 \ \ \%. \tag{4.2}$$

## 5. Power Ratio Error

By ignoring the mismatch factors and the asymmetry ratio, the first-order differential of the radiometer equation with respect to the $Y$ ratios leads to a relative error $\mathcal{E}_y$ in the DUT noise temperature equal to

$$\mathcal{E}_y = \mid 1 - T_a/T_x \mid \delta[(Y_x - 1)/(Y_s - 1)]/[(Y_x - 1)/(Y_s - 1)]. \tag{5.1}$$

Previous tests [9] have shown that the NBS Type IV power bridge [10] is capable of measuring power ratios to better than ±0.002 dB, and that the error is random and independent of the value of the ratio. The test described in reference [9] was repeated (using a non-precision attenuator) on the present radiometer with the 2-4 GHz front end, and resulted in an error of ±0.015 dB (see figure 3). Although it is thought that most of the error appearing in figure 3 is due to the non-precision r.f. attenuator, for the present an error of ±0.01 dB for the uncertainty of the ratio in (5.1) is assumed. This results in a 0.23% error in the last factor of (5.1), and an error in the DUT temperature of

$$\mathcal{E}_y = 0.23 \mid 1 - T_a/T_x \mid \quad \%. \tag{5.2}$$

## 6. Mismatch Factor Error

Approximate expressions for the mismatch factors $M_x$ and $M_s$ can be obtained by using figure 2 and expressing the complex reflection coefficients appearing there in terms of their real ($x$) and imaginary ($y$) parts:

$$\begin{aligned} M_x &\equiv (1 - \mid \Gamma_x \mid^2)(1 - \mid \Gamma_3 \mid^2)/\mid 1 - \Gamma_3\Gamma_x \mid^2 \\ &\doteq 1 - (x_x - x_3)^2 - (y_x + y_3)^2 \end{aligned} \tag{6.1}$$

and

$$\begin{aligned} M_s &\equiv (1 - \mid \Gamma_s \mid^2)(1 - \mid \Gamma_0 \mid^2)/\mid 1 - \Gamma_s\Gamma_0 \mid^2 \\ &\doteq 1 - (x_s - x_0)^2 - (y_s + y_0)^2. \end{aligned} \tag{6.2}$$

Combining these equations leads to

$$M_s/M_x \doteq 1 - (x_s - x_0)^2 - (y_s + y_0)^2 + (x_x - x_3)^2 + (y_x + y_3)^2. \tag{6.3}$$

The relative first-order uncertainty in this ratio is

$$\begin{aligned} \delta[(M_s/M_x)]/(M_s/M_x) \doteq 2[&(x_x - x_3)(\delta x_x - \delta x_3) - (x_s - x_0)(\delta x_s - \delta x_0) \\ &+ (y_x + y_3)(\delta y_x + \delta y_3) - (y_3 + y_0)(\delta y_s + \delta y_0)]. \end{aligned} \tag{6.4}$$

Numerous 6-port reflectometer measurements at 94 GHz in the WR10 waveguide band and in the 2-4 GHz frequency range indicate that the systematic errors in $x$ and $y$ are less than ±0.005. These values are assumed to apply in the present case until a more complete error analysis of the 6-port measurements can be performed. Assuming the systematic errors to be independent of the magnitude of the real and imaginary parts of the reflection coefficients, only the last two terms of (6.4) survive, leading to

$$\delta[(M_s/M_x)]/(M_s/M_x) = \mid y_x + y_3 - y_s - y_0 \mid \quad \%. \tag{6.5}$$

The form of the radiometer equation shows that the relative error $\mathcal{E}_m$ in $T_x$ due to mismatch uncertainty is given by

$$\mathcal{E}_m = \delta[(M_s/M_x)]/(M_s/M_x). \tag{6.6}$$

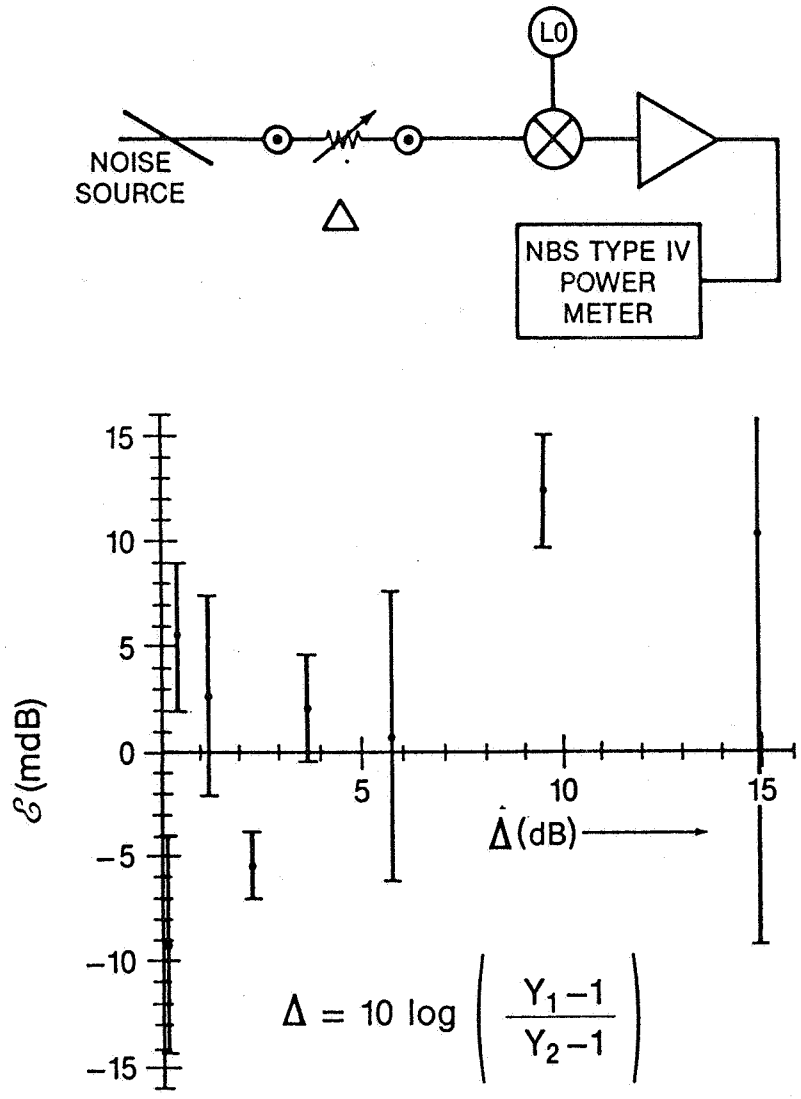


**Figure 3.** The noise source at the top of the figure terminates a precision variable-vane r.f. attenuator. Two $Y$ factors, $Y_1$ and $Y_2$, are determined by the Type-IV power meter for two different settings of the attenuator corresponding to an attenuation difference of $\Delta$ in dB. If the attenuator and power meter are error free, these quantities are related by the equation at the bottom of the figure. The actual error $\mathcal{E}$ is the difference between the left and right hand members of this equation, and is plotted in mdB along the ordinate.

## 7. Asymmetry Measurement and Error

The presence of the efficiency ratio $\eta_s/\eta_x$ in (2.7) is due to the asymmetry in path efficiencies between the path from port 3 (see fig 2) to the receiver and the path from port 0 to the receiver. The measurement of this asymmetry is performed by using two solid-state noise diodes in the setup shown in figures 4a and 4b, which are simplified schematic diagrams of the portion of the system preceding the receiver in figure 2. With diode No. 1 ($T_{x1}$) connected to port 3 (fig 4a) and switches 22, 23, and 25 in the 'up' position, the power

delivered to the receiver is

$$p_{x1} = M_{x1}\eta_x(T_{x1} - T_a) + NT_a + NT_e \tag{7.1}$$

where $M_{x1}$ and $N$ are mismatch factors at the ports shown, $T_a$ is the ambient temperature of the two switches and the isolator, and $NT_e$ is the effective input noise temperature of the receiver. Sufficient isolation is present to insure that the mismatch factor at the isolator-receiver junction remains constant, independent of the switch positions. With switches 23 and 24 'down'

$$p_{x2} = M_{x2}\eta_s(T_{x2} - T_a) + NT_a + NT_e \tag{7.2}$$

and with switch 22 'down'

$$p_a = NT_a + NT_e. \tag{7.3}$$

Equations (7.1), (7.2), and (7.3) can be combined to give

$$\eta_s/\eta_x = (M_{x1}/M_{x2})[T_{x1} - T_a)/(T_{x2} - T_a)](Y_{x2} - 1)/(Y_{x1} - 1) \tag{7.4}$$

where $Y_{x1}$ is the measured ratio of $p_{x2}$ to $p_a$, and $Y_{x2}$ is the ratio of $p_{x1}$ to $p_a$.

The two noise diodes are interchanged and the process repeated (fig 4b), yielding

$$\eta_s/\eta_x = (M'_{x2}/M'_{x1})[(T_{x2} - T_a)/(T_{x1} - T_a)](Y'_{x1} - 1)/(Y'_{x2} - 1) \tag{7.5}$$

where $Y'_{x1}$ is the ratio of $p'_{x1}$ to $p_a$, and $Y'_{x2}$ is the ratio of $p'_{x2}$ to $p_a$.

After multiplying (7.4) and (7.5) together and taking the square root,

$$\eta_s/\eta_x = \{[M_{x1}M'_{x2}/M_{x2}M'_{x1}](Y_{x2} - 1)(Y'_{x1} - 1)/[(Y_{x1} - 1)(Y'_{x2} - 1)]\}^{1/2}. \tag{7.6}$$

Equation (7.6) is used to determine the path-asymmetry ratio, with the mismatch factors determined by 6-port reflectometer measurements.

The relative error $\mathcal{E}_{as}$ in the DUT noise temperature can be estimated by taking the first-order differential of (7.6) with respect to the asymmetry ratio, and leads to

$$\begin{aligned} \mathcal{E}_{as} &= \mid 1 - T_a/T_x \mid \delta(\eta_s/\eta_x) \\ &= 0.23 \mid 1 - T_a/T_x \mid \delta\Delta \ \ \% \end{aligned} \tag{7.7}$$

where $\delta\Delta$ is the dB uncertainty in the asymmetry ratio.

$\Delta$ (see fig 3) has only been estimated for the 2-4 GHz band, resulting in a value of $\pm$ 0.01 dB. This value was determined from the following three pieces of information: 1) when the asymmetry ratio was measured at 100 MHz steps across the 2-4 GHz frequency range it was found to lie within a $\pm$ 0.01 dB spread ($\eta_s/\eta_x$ within the range from 0.998 to 1.002) and to be randomly distributed; 2) when the attenuation of a 3 dB pad was measured by performing an asymmetry measurement with and without the pad at one of the ports its value was within 0.01 dB of the value measured by a dual 6-port ANA; and 3) when a noise diode was calibrated with and without the 3 dB pad between the diode and the system input, the resulting noise temperatures ($\sim$ 10000 K) agreed to within 10 K. If this entire 10 K difference were attributed to asymmetry ratio uncertainty the uncertainty would be less than 0.004 dB. Therefore, (7.7) with a ($\delta\Delta$) of $\pm$0.01 dB for the 2-4 GHz frequency range appears to be safe and leads to

$$\mathcal{E}_{as} = 0.23 \mid 1 - T_a/T_x \mid \ \ \%. \tag{7.8}$$

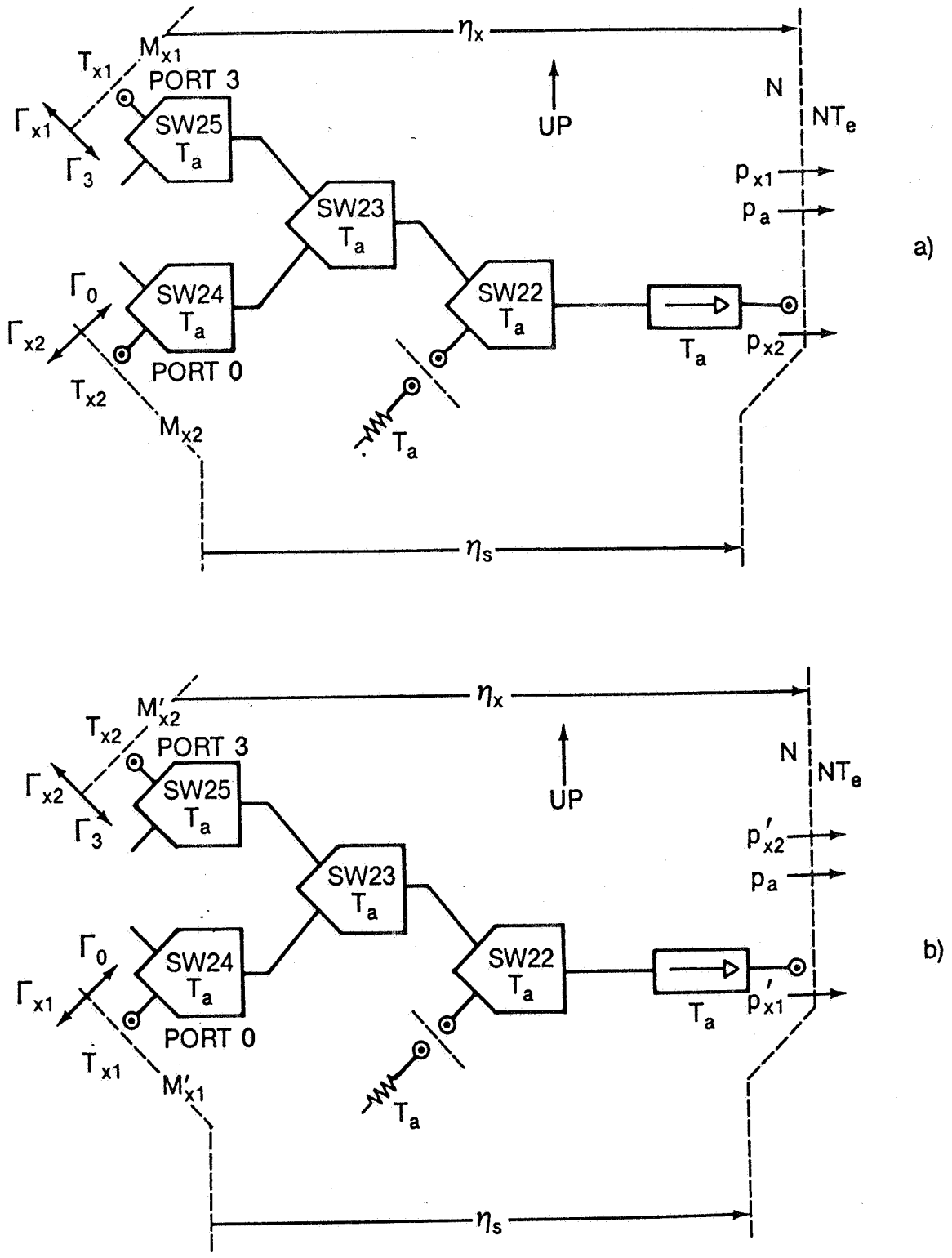


**Figures 4.** A simplified schematic diagram of the radiometer front end with a) diode 1 at port 3 and diode 2 at port 0; and with b) diode 2 at port 3 and diode 1 at port 0.

## 8. Isolation Error

The impedance seen by the receiver changes slightly due to the finite isolation of the isolator in figure 2 as the noise sources $T_x$, $T_a$ and $T_s$ are connected to the system. The receiver noise contributions $N_xT_e$, $N_aT_e$, and $N_sT_e$ vary correspondingly. The resulting error in the DUT noise temperature is calculated from (2.8), (2.9) and (2.10). The error due to a changing mismatch factor, (2.9), is estimated first.

The mismatch factor at the isolator-receiver connector for a particular switch arrangement where source i (i=x, a,or s) is connected to the receiver is

$$N_i = (1-\mid \Gamma_{2i} \mid^2)(1-\mid \Gamma_r \mid^2)/\mid 1-\Gamma_{2i}\Gamma_r \mid^2 . \tag{8.1}$$

The reflection coefficient looking back into the isolator is approximated by the equation

$$\Gamma_{2i} = S_{22} + S_{12}S_{21}\Gamma_i \tag{8.2}$$

where the S's are the scattering coefficients of the switch-isolator combination which are assumed to be independent of switch position. The squared magnitude of this equation is approximately

$$\mid \Gamma_{2i} \mid^2 = \mid S_{22} \mid^2 + 2\,\mathrm{Re}S_{22}^*S_{12}S_{21}\Gamma_i \tag{8.3}$$

where the asterisk indicates the complex conjugate. Equation (8.1) shows that the change in $N$ when source $i$ is replaced by source $j$ is

$$\begin{aligned}\Delta N_{ij} &\equiv N_i - N_j \\ &= \mid \Gamma_{2j} \mid^2 - \mid \Gamma_{2i} \mid^2 + 2\,\mathrm{Re}\Gamma_r(\Gamma_{2i} - \Gamma_{2j}).\end{aligned} \tag{8.4}$$

In terms of (8.2) and (8.3), (8.4) becomes

$$\Delta N_{ij} = 2\,\mathrm{Re}S_{12}S_{21}(\Gamma_r - S_{22}^*)(\Gamma_i - \Gamma_j). \tag{8.5}$$

Using this equation in equation (2.9) yields the approximation

$$\begin{aligned}(\Delta T_x)_N = {} & 2T_a[(T_x - T_a)/(T_s - T_a)]\,\mathrm{Re}S_{12}S_{21}(\Gamma_r - S_{22}^*)(\Gamma_s - \Gamma_a) \\ & + \mathrm{Re}S_{12}S_{21}(\Gamma_r - S_{22}^*)(\Gamma_a - \Gamma_x).\end{aligned} \tag{8.6}$$

Before reducing this error further it will be combined with the error due to changing receiver noise to be estimated next.

The effective temperature (power) delivered to the receiver input which accounts for the noise generated in the receiver itself can be expressed in the form [11]

$$NT_e = T_1 + T_2 \mid \Gamma_2 - \gamma^* \mid^2 \tag{8.7}$$

where $T_1$ and $T_2$ are effective temperatures and where $\gamma^*$ is a complex constant. Each of these are determined experimentally. $\Gamma_2$ represents any of the reflection coefficients $\Gamma_{2x}$, $\Gamma_{2a}$, or $\Gamma_{2s}$. With a change from source i to source j,

$$\begin{aligned}\Delta NT_{eij} &\equiv (NT_e)_i - (NT_e)_j \\ &= T_2(\mid \Gamma_{2i} - \gamma^* \mid^2 - \mid \Gamma_{2j} - \gamma^* \mid^2) \\ &= T_2[\mid \Gamma_{2i} \mid^2 - \mid \Gamma_{2j} \mid^2 - 2\,\mathrm{Re}\gamma^*(\gamma_{2i} - \gamma_{2j})].\end{aligned} \tag{8.8}$$

Using (8.2) in the last equation gives

$$\Delta NT_{eij} = 2T_2 \,\mathrm{Re} S_{12} S_{21} (S_{22}^* - \gamma^*)(\Gamma_i - \Gamma_j) \tag{8.9}$$

and the corresponding DUT error becomes

$$\begin{aligned}(\Delta T_x)_e = 2T_2[((T_x - T_a)/(T_s - T_a))\,\mathrm{Re} S_{12} S_{21} (S_{22}^* - \gamma^*)(\Gamma_s - \Gamma_a) \\ + \mathrm{Re} S_{12} S_{21} (S_{22}^* - \gamma^*)(\Gamma_a - \Gamma_x)].\end{aligned} \tag{8.10}$$

Combining (8.6) and (8.10) leads to

$$\begin{aligned}(\Delta T_x)_{ISO} = 2\,\mathrm{Re}\{[(T_2 - T_a)S_{22}^* + T_a T_r - T_2\gamma^*] \\ \cdot [(T_x - T_a)\Gamma_s/(T_s - T_a) + (T_s - T_x)\Gamma_a/(T_s - T_a) - \Gamma_x]\}.\end{aligned} \tag{8.11}$$

Noting that $\mid S_{21} \mid$ is approximately 1, and taking the maximum possible value of the right-hand side of (8.11) leads to

$$\begin{aligned}(\Delta T_x)_{ISO} \equiv 2 \mid S_{12} \mid \{[\mid S_{22} \mid\mid T_2 - T_a \mid + T_a \mid \Gamma_r \mid + T_2 \mid \gamma^* \mid] \\ \cdot [\mid (T_x - T_a)/(T_s - T_a) \mid\mid \Gamma_s \mid + \mid (T_x - T_a)/(T_s - T_a) \mid\mid \Gamma_a \mid + \mid \Gamma_x \mid]\}.\end{aligned} \tag{8.12}$$

Previous measurements [11] and the fact that the effective input noise temperature of the automated radiometer is approximately 1000 K lead to the following values : $T_2 = 500$ K and $\mid \gamma^* \mid = 0.25$. The assumed isolator parameters are $\mid S_{21} \mid \sim 0.003$ (corresponding to three isolators with a total minimum isolation of 50 dB) and $\mid S_{22} \mid = 0.1$. A value of 0.1 for $\mid \Gamma_r \mid$ and $\mid \Gamma_a \mid$, 300 K for $T_a$, and 77 K for $T_s$ are also assumed. With these values and (8.12), the relative error $\mathcal{E}_i$ in the DUT noise temperature due to finite isolation is

$$\mathcal{E}_i \equiv (\Delta T_x)_{ISO}/T_x = 0.47 \mid \Gamma_s \mid\mid 1 - T_a/T_x \mid + 0.047 \mid 1 - T_s/T_x \mid + 100 \mid \Gamma_x \mid / T_x \ \ \%. \tag{8.13}$$

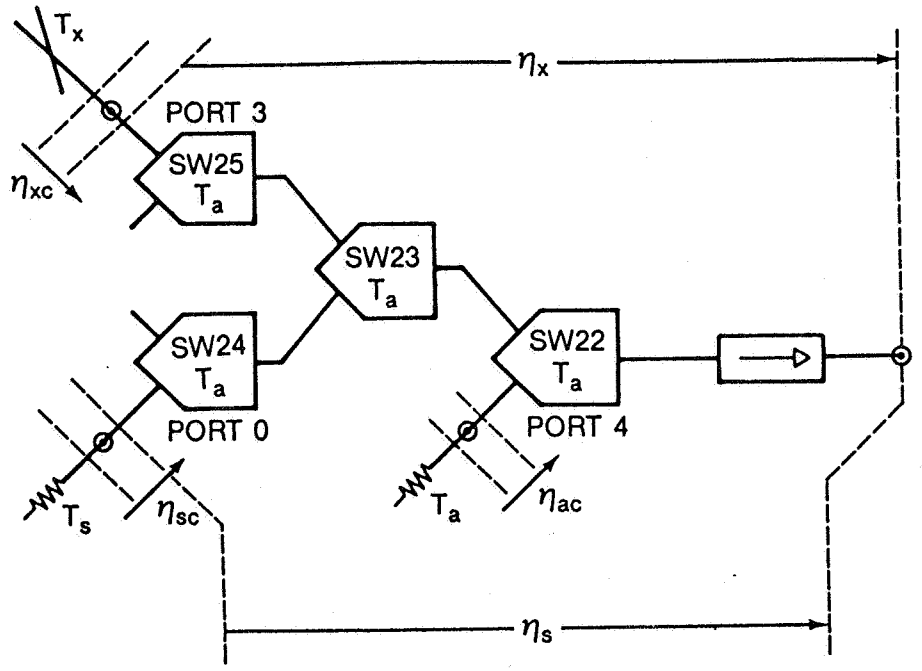


**Figure 5.** A schematic diagram indicating the connector efficiencies $\eta_{xc}$, $\eta_{sc}$, and $\eta_{ac}$ at the DUT, cryogenic, and ambient ports respectively.

## 9. Connector Error

Ideal connectors at the system input ports have been assumed in the development of the radiometer equation. To insure low loss and high repeatability at these ports, the highest quality connectors are used on the system and on the ambient and cryogenic standards. To see how imperfect connectors affect the noise measurement consider figure 5, where $\eta_{xc}$, $\eta_{ac}$, and $\eta_{sc}$ are the connector efficiencies at the DUT, ambient, and cryogenic standard ports respectively. A development similar to that of section 2 reveals a modified radiometer equation of the form

$$T_x = T_a + (M_s/M_x)(\eta_s/\eta_x)[(Y_x - 1)/(Y_s - 1)](T_s - T_a)(\eta_{sc}/\eta_{sx}). \tag{9.1}$$

This differs from the radiometer equation (2.7) for ideal connectors by the presence of the last factor $\eta_{sc}/\eta_{cx}$. The efficiency of the ambient termination connector pair is absent from this equation because the switches and this termination are at the same temperature. Comparison of (9.1) and (2.7) leads to the following expression for the relative DUT noise temperature error due to ignoring the last factor in (9.1):

$$\mathcal{E}_c = \mid \eta_{sc}/\eta_{xc} - 1 \mid . \tag{9.2}$$

This error consists of a systematic part which accounts for the fact that the DUT connector may have a different metallic conductivity or contact resistance than the cryogenic standard, and a random part accounting for connector non-repeatability. The non-repeatability component is included with the systematic component because the sources remain connected to the system throughout a complete calibration procedure.

Connector repeatability is an incompletely explored subject at the present time so a final analysis of

non-repeatability error is not possible. Therefore, what follows is a temporary estimate to be updated when a better treatment is available. Thirteen sets of measurements of the DUT noise temperature were made at 3 GHz with the standard and DUT noise sources being removed and reattached to the system between each set, each set containing 100 DUT noise temperature determinations. The standard deviation of the mean was estimated for the 100 points of each of the 13 sets, the average of which was 15.7 K. This is the amount of inherent random fluctuation to be expected. The standard deviation of the 13 data points was 24.4 K. Assuming that 15.7 K of this value is due to the inherent fluctuations, the remaining 8.7 K (24.4-15.7) is due to connector non-repeatability. This value is 0.087% of the average DUT noise temperature at 3 GHz. The value appropriate for other frequencies is obtained by multiplying by $(f/3)^{1/2}$ since connector loss is assumed to vary as the square root of the frequency. Therefore, the relative DUT noise temperature error due to connector non-repeatability is $0.050 f^{1/2}$ % where $f$ is the frequency in GHz.

The maximum relative DUT noise temperature error due to the DUT and system conductivities being different is given by the expression

$$0.035 f^{1/2} \mid 1 - T_a/T_x \mid \quad \% \tag{9.3}$$

where $f$ is the frequency in GHz. Combining this error with the non-repeatability error leads to

$$\mathcal{E}_c = 0.050 f^{1/2} + 0.035 f^{1/2} \mid 1 - T_a/T_x \mid \quad \%. \tag{9.4}$$

The noise temperatures for the ambient and cryogenic noise standards, $T_a$ and $T_s$, are referenced to the planes immediately preceding their respective connectors. As a result, the connector losses are included as part of the radiometer during the DUT noise temperature measurement as is the DUT connector loss when the DUT is connected to the system. Therefore, the DUT noise temperature $T_x$ is referred to a plane just preceding the DUT connector, and does not include the connector noise contribution. This way of defining the reference planes is the most useful since connector losses are variable and usually ignored in practice.

## 10. Frequency Offset Error

The noise measurement system employs a superheterodyne receiver which, due to the broad-spectrum character of the noise signal, selects upper and lower sidebands around the local oscillator (LO) frequency for processing. In addition, the efficiency ratio (see (2.7)) is also determined in this mode of operation. The mismatch factor ratio, however, is determined by operating the system in its reflectometer mode where the various reflection coefficients making up the mismatch factors (see (6.1) and (6.2)) are determined at the calibration frequency, not the LO sideband frequencies. This ordinarily causes no measurable error unless there is a long transmission line between the system input ports and the isolator in figure 2. If this length is denoted by $\ell$ (the length from port 0 or port 3 to the isolator) the relative error $\mathcal{E}_o$ in the DUT noise temperature is

$$\begin{aligned}\mathcal{E}_o = 200 \mid \cos(4\pi f\ell/30)\,\mathrm{sinc}(\pi B\ell/15) - 1 \mid (\mid \Gamma_s \mid + \mid \Gamma_x \mid) \\ \cdot \mid s_{11} \mid\mid 1 - T_a/T_x \mid \quad \%\end{aligned} \tag{10.1}$$

where $f$ is the i.f. frequency in GHz, $\ell$ is the length in centimeters, B is the i.f. frequency bandwidth in GHz, "sinc" stands for $\sin(x)/x$, and $s_{11}$ is the isolator input reflection coefficient. For a $f, \ell, B$, and $\mid s_{11} \mid$ of 0.03 GHz, 15 cm, 0.01 GHz, and 0.1 respectively

$$\mathcal{E}_o = 0.36(\mid \Gamma_s \mid + \mid \Gamma_x \mid) \mid 1 - T_a/T_x \mid \quad \%. \tag{10.2}$$

## 11. Nonlinearity Error

There are three nonlinearities in the radiometer: mixer nonlinearity; amplifier compression; and nonlinearities in the thermistor mount used to detect the radiometer output power. Mixer nonlinearity refers to a mixer i.f. output which contains exponents of the r.f. signal (the signal in the present case is the wave amplitude from a noise source connected to the input of the radiometer) greater than the first power. A simple analysis [12] shows that the next exponent to appear after the first in the i.f. output can be no less than the third power . Assuming this exponent to be present, its coefficient would be proportional to $(P_s/P_{lo})^{3/2}$ where $P_s$ and $P_{lo}$ are the signal and local oscillator powers respectively. For a noise source with a $10^4$ K noise temperature, a local oscillator power of 1 mW, and a system noise bandwidth of $10^7$ Hz, this coefficient is of the order of $10^{-14}$. The resulting error in the measured DUT noise temperature is insignificant.

The DUT noise temperature error caused by amplifier compression and power meter nonlinearities are accounted for by treating both together as a variable gain (a gain which is a function of an input power). The resulting nonlinearity constant $aBG$ (to be defined in a moment) is a measure of this system nonlinearity and is carefully determined for the system before any noise calibrations are performed, and then carried in computer memory for later error calculations. Figure 6 is a schematic diagram of the model used to develop the error equation, and consists of three noise sources, an r.f. amplifier and mixer, a local oscillator, an i.f. attenuator and amplifier, and a power meter. The noise temperatures of the DUT, ambient, and cryogenic sources are $T_x$, $T_a$, and $T_s$ respectively. The r.f. and i.f. amplifiers have effective input noise temperatures of $T_{e1}$ and $T_{e2}$ , and the gain of the r.f. amplifier is $g_1$. The i.f. amplifier gain is variable and assumes the form $g_2/(1 + ag_2q/k)$, where $g_2$ is the gain of a fictitious amplifier in which the constant $a$ vanishes. The input and output powers of the i.f. amplifier are $q$ and $p$, and $k$ is Boltzmann's constant. $T_a$ and $\beta$ are the ambient temperature and efficiency of the variable attenuator between the two amplifiers.

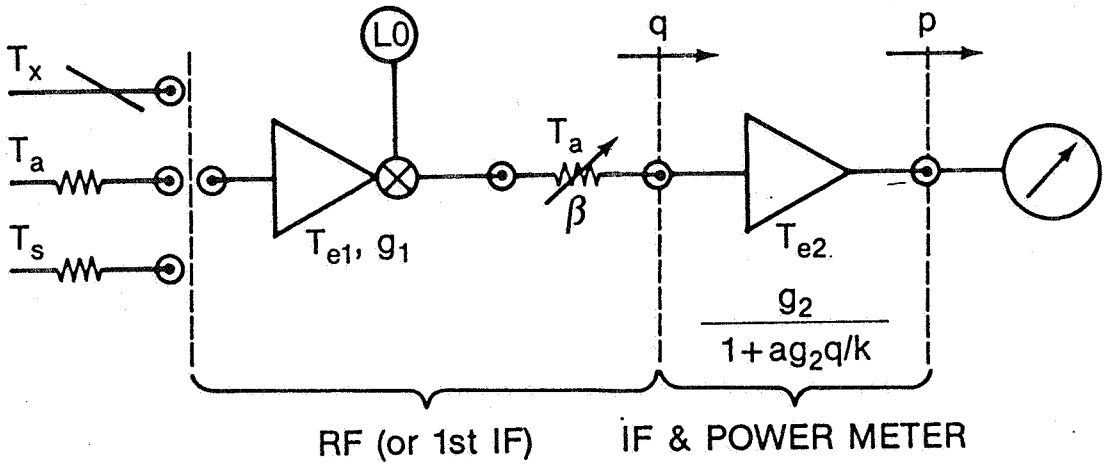


**Figure 6.** A schematic diagram of the r.f. and i.f. portions of the automated radiometer.

The input power $q$ is

$$q = kBg_1\beta(T + T_e) \tag{11.1}$$

where the system effective input noise temperature referred to the r.f. amplifier input port is

$$T_e \equiv T_{e1} + [T_a(1-\beta) + T_{e2}]/g_1\beta \ . \tag{11.2}$$

The $g_1\beta$ factor in the denominator of (11.2) remains large enough during the nonlinearity measurement ($\beta$ is changed as part of the measurement process) to assume that $T_e$ is constant and equal to $T_{e1}$. The output power $p$ detected by the power meter is related to $q$ by the formula in the figure which leads to

$$p = kBG(T + T_e)/[1 + aBG(T + T_e)] \tag{11.3}$$

where

$$G \equiv g_1\beta g_2. \tag{11.4}$$

Denoting the powers with the various noise sources connected to the radiometer input by $p_x$, $p_a$, and $p_s$, and using (11.3) leads to

$$\begin{aligned} T_x - T_a = (T_s - T_a)[(Y_x - 1)/(Y_s - 1)] \\ \cdot \{[1 + aBG(T_x + T_e)]/[1 + aBG(T_s + T_e)]\} \end{aligned} \tag{11.5}$$

where

$$Y_x = p_x/p_a \tag{11.6}$$

and

$$Y_s = p_s/p_a \tag{11.7}$$

are the $Y$ factors determined from the power measurements. Equation (11.5) is an "exact" formula between the noise temperatures that includes the variable gain of the system. The formula used to estimate the DUT temperature is

$$\hat{T}_x - T_a \equiv (T_s - T_a)(Y_x - 1)/(Y_s - 1) \tag{11.8}$$

where $\hat{T}_x$ is the estimated temperature. Combining (11.5) and (11.8) leads to the approximation

$$T_x \doteq \hat{T}_x + (\hat{T}_x - T_a)(\hat{T}_x - T_s)aBG \tag{11.9}$$

relating the true DUT temperature $T_x$ and the estimated temperature, where the nonlinearity constant $aBG$ is small and accounts for amplifier compression and power meter nonlinearity. Amplifier compression makes the constant $a$ in this last equation positive while the power meter nonlinearity causes a negative $a$. Therefore, the product $aBG$ can be positive or negative.

The constant $aBG$ corresponds to an optimum value (a value that gives a minimum for $a$) of $\beta$ determined during the nonlinearity measurement, and is used in subsequent noise temperature measurements. Once $\beta$ is set and a measurement is made to determine an approximate value for the corresponding DUT noise temperature $\hat{T}$, a value for $aBG$ can be found by making two more measurements of the DUT temperature, $\hat{T}_1$ and $\hat{T}_2$, for two different values for the i.f. attenuator efficiency, $\beta_1$ and $\beta_2$. The constant can then be calculated from

$$aBG = C(\hat{T}_1 - \hat{T}_2)/(\beta_1 - \beta_2) \tag{11.10}$$

where

$$C \equiv 1/[(\hat{T} - Y_a)(\hat{T} - T_s)]. \tag{11.11}$$

This measurement is repeated 50 to 100 times and an average calculated. Another pair of $\beta$'s is chosen and another average determined, eventually covering a 3 dB range on both sides of the optimum $\beta$ in steps of 1 dB. An average ($\overline{aBG}$) and an estimated standard error of the mean ($SEM$) for the collection of preceding averages is then calculated.

The DUT noise temperature is estimated ($\hat{T}_x$) from (11.8) while (11.9) shows that this estimate differs from the "true" DUT temperature ($T_x$) by the amount equal to the second term of (11.9). The resulting error in the DUT temperature is

$$\mathcal{E}_n = \mid (\hat{T}_x - T_a)(\hat{T}_x - T_s) \mid \epsilon_n/\hat{T}_x \tag{11.12}$$

where

$$\epsilon_n = \mid \overline{aBG} \mid + 0.64SEM. \tag{11.13}$$

The second term in (11.13) assures that there is less than a 10% probability that the error is greater than stated if the distribution of the averages leading to $\overline{aBG}$ is normal. The current value of $\epsilon_n$ is $1.42 \times 10^{-8}$. A previous determination gave the value of $1.55 \times 10^{-8}$. To monitor the system linearity an attenuator at the input (the one shown in fig 6) and output (not shown in the figure) of the second i.f. amplifier are switched an equal amount and the output powers checked to insure that the two powers are equal. If the

values obtained are within 1 part in $10^4$, the system is behaving properly. Inserting the value $1.42 \times 10^{-8}$ into (11.12) yields

$$\mathcal{E}_n = 1.42 \times 10^{-6} \mid (\hat{T}_x - T_a)(\hat{T}_x - T_s) \mid / \hat{T}_x \ \ \%. \tag{11.14}$$

Check standards are also used to monitor the overall system performance.

## 12. Total Error

The total systematic error is the linear sum of the error components discussed in §3 through §11, and it is assumed that the true value of the DUT noise temperature lies within the range given by the noise temperature calculated from the radiometer equation plus or minus this total error (assuming no random errors).

$$\begin{aligned} E_t \equiv \mathcal{E}_s + \mathcal{E}_a + \mathcal{E}_y + \mathcal{E}_m + \mathcal{E}_{as} \\ + \mathcal{E}_i + \mathcal{E}_c + \mathcal{E}_o + \mathcal{E}_n \ . \end{aligned} \tag{12.1}$$

An unweighted root-sum-square (rss) error $E_{rss}$ is also defined, where dependent errors are summed linearly before the rss calculation is performed. Only $\mathcal{E}_Y$, $\mathcal{E}_m$, and $\mathcal{E}_{as}$ are interdependent, so the definition leads to

$$\begin{aligned} E_{rss} \equiv [\mathcal{E}_s^2 + \mathcal{E}_a^2 + (\mathcal{E}_y + \mathcal{E}_m + \mathcal{E}_{as})^2 + \mathcal{E}_i^2 \\ + \mathcal{E}_c^2 + \mathcal{E}_o^2 + \mathcal{E}_n^2]^{1/2}. \end{aligned} \tag{12.2}$$

A typical set of error components is shown in Table 1 for a frequency of 3 GHz and a DUT noise temperature of 11000 K. The true error is less than the total error (1.72%) at the bottom of the table.

The systematic error for the 1–12 GHz coaxial system at 3 GHz as a function of DUT noise temperature is shown in figure 7. Figure 8 shows the error as a function of frequency. The thick portions of the linear and rss curves are a reminder that the measurements leading to these two figures and the table were performed with the 2-4 GHz front end. Measurements with the other front ends, when available, are expected to yield error limits close to the dashed portions of the two curves in figure 8. The systematic errors for the millimeterwave systems will be similar to those in the figures.

Table 1. A typical set of systematic errors at 3 GHz for a DUT noise temperature of 11000 K. The source errors in column two are explained in the text. Column three shows the resulting % errors in the DUT noise temperature.

| DUT NOISE TEMPERATURE ERROR | | |
|---|---|---|
| Frequency = 3 GHz | Noise Temp = 11000 kelvin | |
| *Source* | *Source Error* | *± % Error in $T_x$* |
| $T_m$ | eq (3.2) | 0.64 |
| $T_a$ | 0.25 K | 0.17 |
| Mismatch | 0.005 | 0.14 |
| Asymmetry | 0.01 dB | 0.22 |
| Isolation | 50 dB | 0.09 |
| Connector | $0.05 f^{1/2}$ | 0.15 |
| Offset | eq (10.1) | 0.07 |
| Nonlinearity | $1.42 * 10^{-8}$ | 0.02 |
| Total Error (linear sum) | | 1.72 |
| RSS Error | | 0.90 |

## 13. Summary, Discussion, and Conclusions

A noise measurement with the NIST automated radiometer employs the radiometer equation (2.7) to estimate the noise temperature of a device under test from the calculated ambient and cryogenic noise temperatures, and the measured Y's, M's, and $\eta$'s. The associated errors are summarized in figures 7 and 8 and Table 1, and are discussed in sections 3 thru 12.

Of the few questions still to be answered by future measurements, however, connector error presents the greatest uncertainty. The $0.05 f^{1/2}$ % error assumed in section 9 for this error is ad hoc at best, and needs more investigation.

The cryogenic standard has been implemented with both a type-N male and an APC 7 mm connector, so the devices to be tested must have one of these two types of connectors.

Operationally, the radiometer is one of the most stable in existence, and in conjunction with the cryogenic standard produces very repeatable results [2].

## 14. Acknowledgments

Both the configuration and implementation of the NIST automated radiometer covers a significant time span and has involved a number of contributors. Among the more important are G. J. Counas, L. D. Driver, C. K. S. Miller, G. R. Reeve, D. F. Wait, and J. Wakefield.

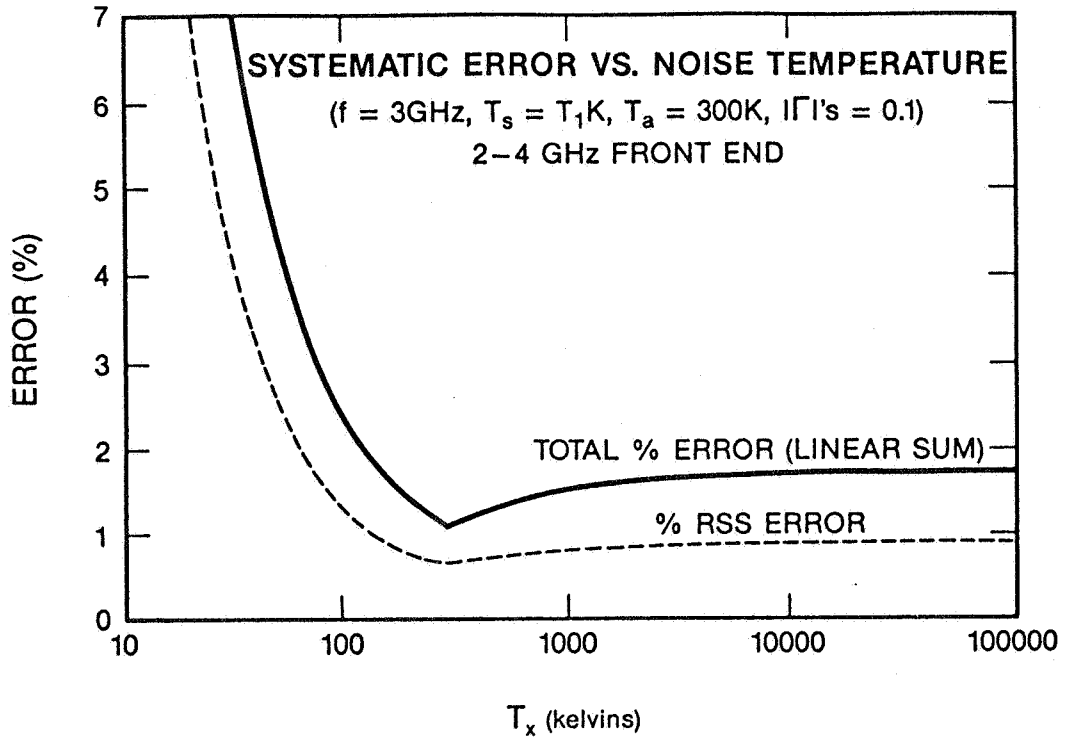


**Figure 7.** Systematic error as a function of DUT noise temperature at 3 GHz assuming 0.1 reflection coefficients for the noise sources and radiometer input ports.

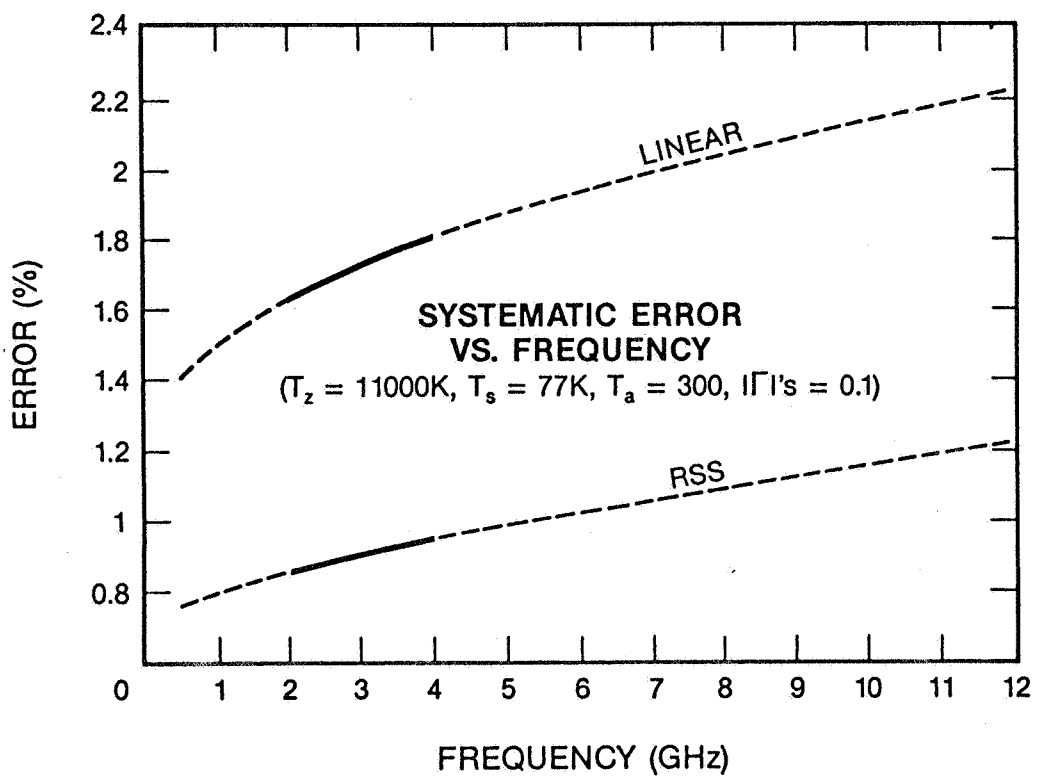


**Figure 8.** Systematic error as a function of frequency for a DUT noise temperature of 11000 K and 0.1 reflection coefficients.

## 15. References


[1] Miller, C. K. S.; Daywitt,W. C. The NBS switching radiometers. Nat. Bur. Stand. (U.S.) NBSIR–3004; 1984 May.

[2] Counas, G. J. 2.0 GHz to 4.0 GHz automated radiometer—operation and service manual. Nat. Bur. Stand. (U.S.) NBSIR 83–1697; 1984 January.

[3] IEEE Standard Dictionary of Electrical and Electronic Terms. New York, N. Y.; Wiley–Interscience, a division of John Wiley and Sons, Inc.;1972.

[4] Miller, C. K. S.; Daywitt, W. C.;Arthur, M. C. Noise standards, measurements, and receiver noise definitions. Proc. IEEE, Vol. 55, No. 6: 865–877; 1967 June.

[5] Wells, J. S.; Daywitt, W. C.;Miller, C. K. S. Measurement of effective temperatures of microwave noise sources. IEEE Trans. on I&M, IM–3: 17–18;1984 March.

[6] Wait, D. F. The sensitivity of the Dicke Radiometer. J. Res. Nat. Bur. Stand. (U.S.) – C. Eng. and Inst.,Vol. 71C, No. 2,1967 April.

[7] Mumford, W. W.; Scheibe, E. H. Noise Performance Factors in Communications Systems. Dedham, Massachusetts: Horizon House–Microwave, Inc.; 1962.

[8a] Daywitt, W. C. A coaxial noise source for the 1 GHz to 12.4 GHz frequency range. Nat. Bur. Stand. (U.S.) TN 1074; 1984 March.

[8b] Daywitt, W. C. Design and Error Analysis for the WR10 Thermal Noise Standard. Nat. Bur. Stand. (U.S.) TN 1071; 1983 December.

[9] Wait, D. F. The impact of automation on NBS noise temperature measurements. Proc. IEEE, Vol.74, No. 1;117–120; 1984 January.

[10] Larsen, N. T. NBS Type–IV power meter, operation and maintenance manual. Nat. Bur. Stand. (U.S.) NBSIR 77–866;1977 October.

[11] Engen, G. F. A new method of characterizing amplifier noise performance. IEEE Trans. on Instr.,IM–19, No.4,344–349;1970 November.

[12] Southworth, G. C. Principles and Applications of Waveguide Transmission. New York, N. Y.; D. Van Nostrand Company, Inc.;1956.

NBS-114A (REV. 2-80)

| U.S. DEPT. OF COMM. **BIBLIOGRAPHIC DATA SHEET** *(See instructions)* | 1. PUBLICATION OR REPORT NO. NIST/TN-1327 | 2. Performing Organ. Report No. | 3. Publication Date March 1989 |
|---|---|---|---|

4. TITLE AND SUBTITLE

Radiometer Equation and Analysis of Systematic Errors for the NIST Automated Radiometers

5. AUTHOR(S)

W. C. Daywitt

6. PERFORMING ORGANIZATION *(If joint or other than NBS, see instructions)*

~~NATIONAL BUREAU OF STANDARDS~~ National Institute of Standards and Technology
DEPARTMENT OF COMMERCE
WASHINGTON, D.C. 20234

7. Contract/Grant No.

8. Type of Report & Period Covered

9. SPONSORING ORGANIZATION NAME AND COMPLETE ADDRESS *(Street, City, State, ZIP)*

10. SUPPLEMENTARY NOTES

☐ Document describes a computer program; SF-185, FIPS Software Summary, is attached.

11. ABSTRACT *(A 200-word or less factual summary of most significant information. If document includes a significant bibliography or literature survey, mention it here)*

Equations used in the NIST coaxial and waveguide automated radiometers to estimate the noise temperature and associated errors of a single-port noise source are derived in this report. These equations form the foundation upon which the microwave and millimeterwave noise calibration and special test services are performed. Results from the 1-12 GHz coaxial radiometer are presented.

12. KEY WORDS *(Six to twelve entries; alphabetical order; capitalize only proper names; and separate key words by semicolons)*

calibration; error analysis; microwave; millimeterwave; noise temperature; radiometer

13. AVAILABILITY

☒ Unlimited
☐ For Official Distribution. Do Not Release to NTIS
☒ Order From Superintendent of Documents, U.S. Government Printing Office, Washington, D.C. 20402.
☐ Order From National Technical Information Service (NTIS), Springfield, VA. 22161

14. NO. OF PRINTED PAGES

28

15. Price